# Molarities Concentration Effects On Some Characterization Of ($Fe_2O_3$) Thin Film Solar Cell Application

**Majid H. Hassoni, Noor J. Sahib**
Physics Department, Education Faculty,
University of Al- Mustansiriyah, Baghdad, Iraq

**Corresponding author, E-mail:** ahmed_naji_abd@yahoo.com

***Abstract*—In this research study the effect of molarities concentration on the characteristics of films ferric oxide ($Fe_2O_3$) which prepared by Chemical Spray pyrolysis (CSP) technique and deposited on silicon substrates used in solar cell is applied to the parameters of the solar cell (short circuit current ($I_{sc}$) , open circuit voltage ($V_{oc}$) , filling factor (F.F) and efficiency of the solar cells (η)). The results showed that the solar cell efficiency increasing with increasing molarity concentration of ($Fe_2O_3$) films, where the value of the efficiency of the solar cell when the molarity concentration (0.1M) greatest value was of (1.398%) , while the value of the solar cell efficiency when the molarity concentration (0.05M) was (1.065%).**

***Keywords—$Fe_2O_3$, solar cell , AFM, Molarities concentration***

## 1. Introduction

Solar cell is a device which converts photons in solar rays to direct-current (DC) and voltage. Solar cells are described as being photovoltaic , the technology is called Solar Photovoltaic (SPV) [1]. Many different photovoltaic technologies are being developed for large-scale solar energy conversion [2].

The use of semiconducting materials in the form of thin films now a day's occupy prominent place in the basic as well as applied research. It is a technologically useful material due to wide band gap of (2.42 eV) , as many devices such as electronic devices including light emitting diodes, single electron transistors and field effect transistor [3] sensors [4] . In this research the energy gap which is approach to the result in the previous speech where the energy gap at concentration (0.05 M) is (2.3eV) , the energy gap at concentration (0.075M) is (2.48eV) and the energy gap at concentration (0.1M) is (2.5eV). Binary oxides $M_2O_3$ , where M is a trivalent metal, crystallize in the corundum structure and occur in n- as well as p-types [5]. In this group, the hematite ($Fe_2O_3$) was selected as a prototype due to its technological use as a catalyst [6] . Iron oxide thin film ($Fe_2O_3$) found in nature as hematite, is one of the most important oxides of transition elements, which is the most stable among all other iron oxides.[7]. This material is characterized of its good thermal constancy at relatively high temperatures, non-toxic, low-cost , numerous, has environmentally friendly properties , The ferric compounds show high paramagnetic properties, which means that the electrons remain unpaired [8]

## 2. Experimental

In a model procedure , (0.811, 1.2165 and 1.622) g of iron (III) chloride anhydrous ($FeCl_3$), 162.2 g/mol Molar mass (purity 97.0% , Sinopharm Chemical Reagent Co. , Ltd) were dissolved in (100 ml) of distilled water. The solution was added into a round-bottom flask with stirring. The color of the solution was brown. The suspension was kept at 75 °C for (15) minutes. The resultant solution was sprayed on silicon substrates at temperature (375˚C) to get the required thin films.

Crystalline wafer of p-type Silicon with resistivity of (2-20) Ω.cm, 508 μm thickness and (100) orientation were used as starting substrates. The substrates were cut into rectangles with areas of (1×1) cm. After chemical treatment,
(0.1 μm) thick Al layers were deposited by using an evaporation method on the backsides of the wafer. Electrochemical etching then perfect in a mixture (1:1) HF(40%) – Ethanol (99.99) at room temperature by using a (Au) electrode (15 $mA/cm^2$) Current density was applied for (fifteen minutes) etching time and the etched area of sample was (0.785 cm2). Silicon substrates lifted from the surface of the heated and cooled after it reaches a temperature to room temperature

Thickness of the samples was measured using the weighting method , by using the relation

$$t = \frac{\Delta W}{\rho \times Area} \qquad (1)$$

Where (t) is the thin film thickness , (ΔW) is the change in weight (The difference between the substrate weight before and after the deposition) , (ρ) The density of the thin film material ($Fe_2O_3$ material density equal to (5.24g $/cm^3$) and Substrate surface area equal (1$cm^2$). where the use of the thickness of ( 350 nm) .

**3. Results and discussion**

**(3-1) X-Ray Diffraction:**

The results of analysis X-ray diffraction showed that the thin films of ($Fe_2O_3$) is multi-crystallizing (Polycrystalline) nature of the type hexagon and the prevailing direction (104), and peaks in the X-ray diffraction diagrams for the films prepared apply and dramatically with the international card (Joint committee on powder diffraction standards) (JCPDS) for ($Fe_2O_3$) with serial number (00-033-0664).

***Table (1) illustrates the portion of the card (JCPDS) and the results obtained from***
***X-ray diffraction of the thin films of ($Fe_2O_3$) prepared at a temperature (375°C) and three concentrations (0.05,0.075 and 0.1) M***

| Sample | 2θ (degr) | $d_{hkl}$ (Å) | Into. (a.u.) | hkl |
|---|---|---|---|---|
| (STEM) | 24.1378 | 3.684 | 22 | 012 |
| | 33.1522 | 2.7 | 100 | 104 |
| | 35.6112 | 2.519 | 76 | 110 |
| | 54.0892 | 1.6941 | 72 | 116 |
| (0.05 M) | 33.1880 | 2.69724 | 100 | 104 |
| | 35.6773 | 2.51455 | 38 | 110 |
| (0.075M) | 24.1792 | 3.67788 | 22 | 012 |
| | 33.1833 | 2.69761 | 100 | 104 |
| | 35.6673 | 2.51523 | 28 | 110 |
| | 54.1031 | 1.69374 | 31 | 116 |
| (0.1 M) | 24.1784 | 3.678 | 22 | 012 |
| | 33.1689 | 2.69875 | 100 | 104 |
| | 35.6478 | 2.51656 | 34 | 110 |
| | 54.0756 | 1.69454 | 29 | 116 |

The figure (1) display that the intensity of ($Fe_2O_3$) thin film which deposited from the higher concentration increasing indicated that the crystallization defects.

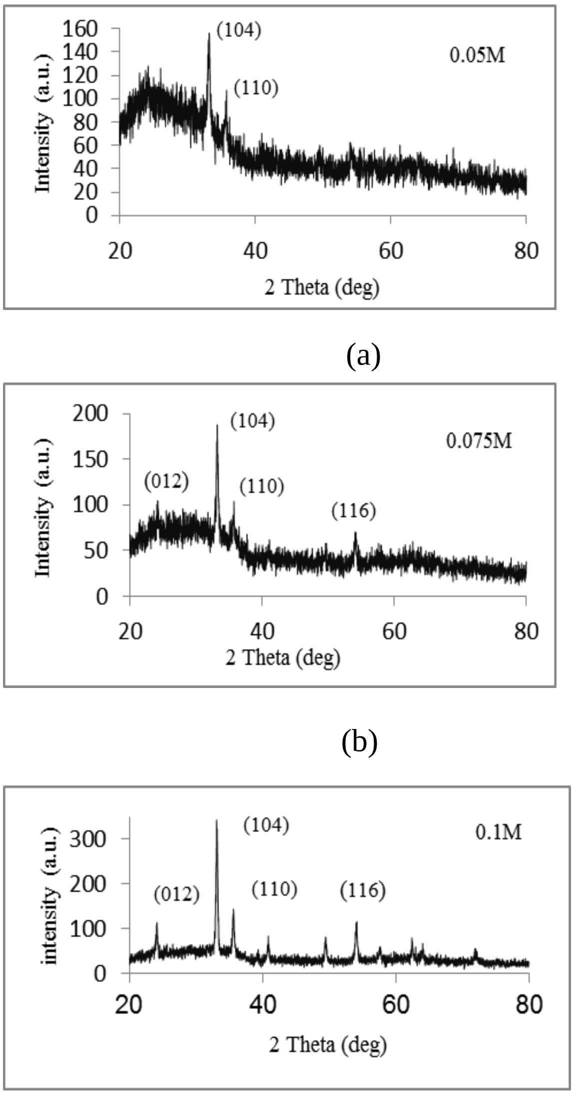


(c)

***Fig.1: XRD patterns of ($Fe_2O_3$) thin films prepared by Chemical Spray pyrolysis (CSP) technique and deposited on glass substrate for three concentrations (0.05, 0.075 and 0.1)M.***

Crystallite size measurements were determined from the full-width at half maximum (FWHM) of the strongest reflection of the (104) peak, using the Scherer approximation, as in equation (2)

$$G = \frac{K\lambda}{\beta \cos\theta} \qquad (2)$$

Where : (G) the Crystallite size ,
(K) the Scherer's constant it's quantity
(0.94) , (λ) the wavelength of the radiation, (β) the full width at half maximum (FWHM) in radians , and
(θ) the Bragg angle.

***Table 2: powder X-ray diffraction data ($Fe_2O_3$) thin film***

| Samples | Crystallite size (nm) | FWHM (deg) |
|---|---|---|
| (0.05 M) | 19.0769 | 0.4167 |
| (0.075 M) | 24.89646 | 0.3193 |
| (0.1 M) | 29.48716 | 0.2696 |

**(2-3)Morphological and Structural Properties of ($Fe_2O_3$) thin film**

In order to study the surface topography of the deposited thin films and the effect of the concentration at the same preparation conditions on it , Atomic force microscope (AFM) was used as it has the ability to produce micrographs and analyze the surface of the samples under investigation to give very precious statistical values of average crystallite size , Roughness average , and the values of the square root of the average square roughness as well as providing us with a lot of important information.

***Table (2) shows the values of roughness average, and the values of the square root of the average square roughness, and the average of crystallite size by measuring the atomic force microscope (AFM) to films prepared.***

| $Fe_2O_3$ Concentration | Roughness average (nm) | RMS (nm) | Average diameter (nm) |
|---|---|---|---|
| (0.05 M) | 4.18 | 5.08 | 67.56 |
| (0.075 M) | 1.04 | 1.25 | 86.83 |
| (0.1 M) | 2.42 | 2.92 | 107.33 |

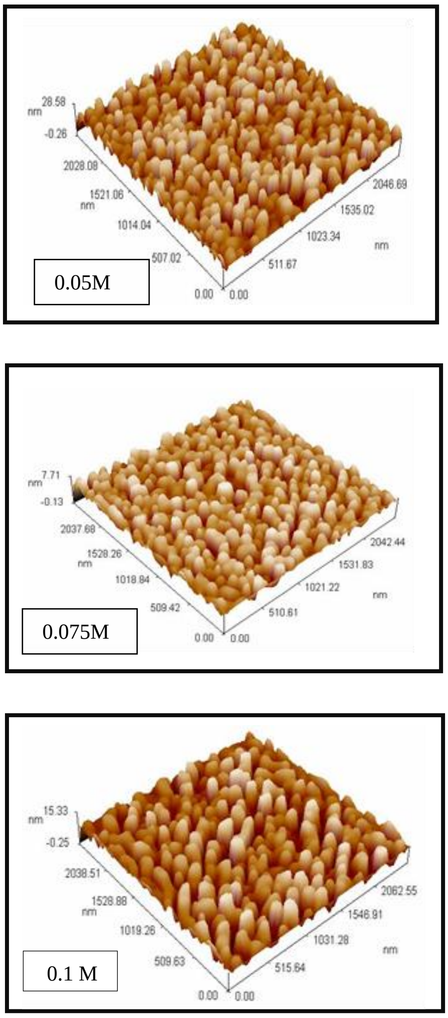


**Fig.2**: ***AFM images of ($Fe_2O_3$) thin films as a function of concentration***

### (3-3) Optical Properties

The figure (3) shows the transmition as a function the wavelength at a range (350-800) nm, also the figure relive that there is no transmittance at the range (350-550) nm. The transmittance started to appear above 550 nm, the increasing in concentration due to decreasing in transmition via that increasing at average grain size.

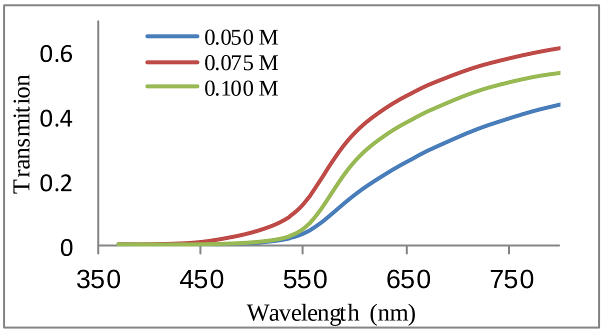


***Fig.3: Transmittance spectrum of ($Fe_2O_3$) thin film which prepared by Chemical Spray pyrolysis (CSP) technique and deposited on glass substrate for three concentration (0.05 , 0.075 and 0.1)M***

The optical absorption coefficient α was evaluated by the relation

$$\alpha h\nu = A(h\nu - E_g)^n \qquad (3)$$

where

$$\alpha = 2.303\,\frac{A}{t} \qquad (4)$$

where (t) is the film thickness and (A) is the absorbency thin film , (hv) is the photon energy , it can be calculated from the relationship

$$E_g = \frac{1240}{\lambda_{(nm)}} \qquad (5)$$

and (n = 0.5) for allowed direct transition. Plotting the graph between [$(\alpha h\nu)^2$] versus photon energy (hv) gives the value of direct band gap. By drawing a straight line touches the curve even goes a photon energy axis at the point $(\alpha h\nu)^2 = 0$ , gives the value of band gap.

Shown in figure (4) the optical band gab is (2.3eV) for concentration (0.0.5M) , (2.48eV) for concentration (0.075M) and (2.5eV) for concentration (0.1M) . This means that whenever the increasing of concentration the value of energy gap increase.

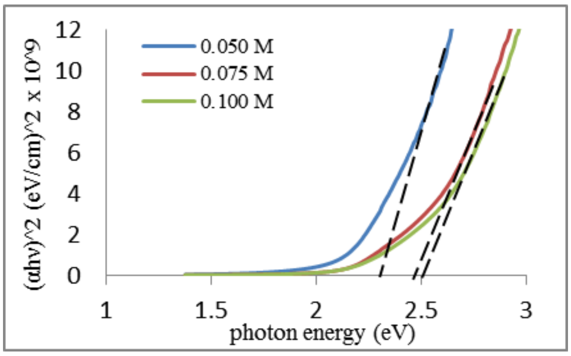


***Fig.4: $(\alpha h\nu)^2$ versus photon energy plot of spectrum of ($Fe_2O_3$) thin film which prepared by Chemical Spray pyrolysis (CSP) technique and deposited on glass substrate for three concentration (0.05 , 0.075 and 0.1)M***

**(4-3) solar cell parameter**

**(1-4-3) I-V properties**

Figures (5) and (6) shows the (I-V) dark characteristics in forward and reverse direction of solar cells heterojunction divider (p-Si /n- $Fe_2O_3$) at temperature (375˚C) and thickness (350nm) and three concentrations (0.05, 0.075, 0.1) M. The forward current of photodetector is very small at voltage less than 2 V. This current is known as *recombination current* which occurs at low voltages only. It is generated when each electron excited form valence band to conductive band. The second region at high voltage represented the diffusion or bending region which depending on serried resistance. In this region; the bias voltage can transmit electrons with enough energy to infiltrate the barrier between the two sides of the junction.

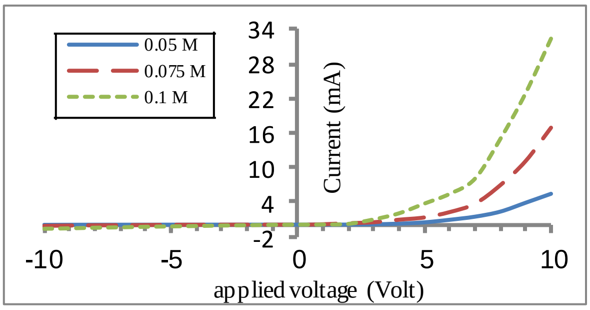


***Fig. 5: I-V characteristic under forward reverse bias of the (p-Si /n- $Fe_2O_3$)***

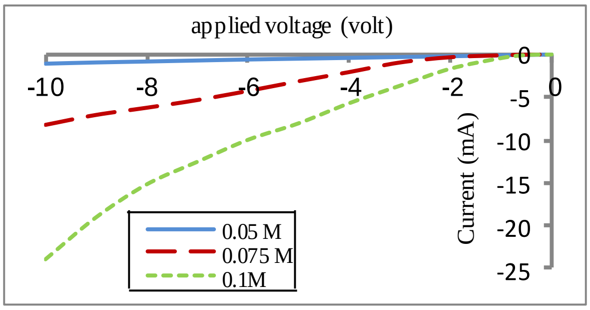


***Fig. 6: illuminated (I-V) characteristic of (p-Si /n- $Fe_2O_3$) photodetectors***

Figure (6) shows that the reversed current-voltage characteristics of the device measured in dark and the photocurrent under a ($41W/m^2$) tungsten lamp illumination .Note of figure (6) having two reversed current, the first area is located within the (2.5 Volt) in the case of concentration (0.05M) , (2 Volt) in the case of concentration (0.075M) and (0.7 Volt) in the case of concentration (0.1M) and the resultant from recombination current, While we note that the second region at high voltage represented the diffusion current. The kind of relating current in to both the front and reverse bias voltages it's linear function.

**(2-4-3) Short Circuit Current and Open Circuit Voltage Measurements**

Both the short circuit current ($I_{sc}$) and open circuit voltage ($V_{oc}$) of the characteristics of the devices, photovoltaic, such as optical detector and solar cells as they describe the efficiency of the device without the need for impartiality or shed an external voltage on the device, and because ($I_{sc}$) and ($V_{oc}$) produce separation of thermocouples (electron - a gap) (np) generated in the depletion region (W) by the internal electric field of the device for the emerging optical radiation fall out without the need to shed external electric field on the device.

Figure (7) has been to find the values of each of the voltage open circuit ($V_{oc}$), and short circuit current ($I_{sc}$) and great voltages ($V_m$) and great current ($I_m$) for three concentrations (0.05, 0.075, 0.1) M has been listed obtained values in the table (3).[9-10]

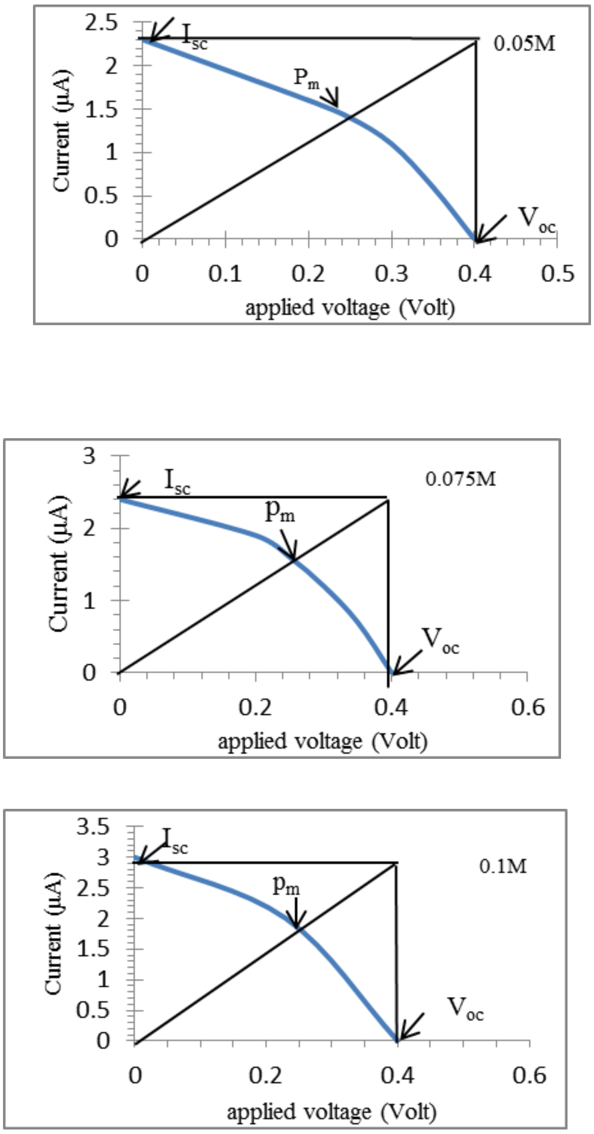


***Fig. 7: illustrates the values of each of the open circuit voltage ($V_{oc}$), short circuit current ($I_{sc}$) , great voltages ($V_m$) and great current ($I_m$) for three concentrations (0.05, 0.075, 0.1) M***

**(3-4-3) Calculation of filling factor and the efficiency of (p-Si/n-$Fe_2O_3$)**

To calculate the value of each of the of filling factor (F.F) and solar cell efficiency (η) for each cell concentrations (0.05, 0.075 and 0.1) M respectively , via the use of two equations

$$F.F = \frac{V_m I_m}{V_{oc} I_{sc}} = \frac{P_m}{V_{oc} I_{sc}} \qquad (6)$$

$$\eta = \frac{P_m}{P_{in}} = \frac{V_{oc} I_{sc} F.F}{P_{in}} \qquad (7)$$

***Table 3: Characterization of solar cell***

| samples | $V_m$ | $I_m$ | $V_{oc}$ | $I_{sc}$ | F.F | η% |
|---|---|---|---|---|---|---|
| 0.05M | 0.245 | 1.4 | 0.4 | 2.3 | 0.372826 | 1.065714 |
| 0.075M | 0.261 | 1.5 | 0.4 | 2.4 | 0.407813 | 1.216405 |
| 0.1M | 0.25 | 1.8 | 0.4 | 2.9 | 0.387931 | 1.398167 |

**4. Conclusions**

Preparation of (Fe2O3) thin films using chemical spray pyrolysis method at different concentration. The results of

X-ray diffraction measurements showed that the thin films of (Fe2O3) prepared at three concentrations (0.05 , 0.075 and 0.1) M were polycrystalline and have hexagonal structure of the type

(□-Fe2O3). The favorite crystal growth for all prepared thin films is (104). The increasing in the concentration of the solution leads to increase in the size of the crystalline grains and improves the crystal structure. The results of the atomic force microscope (AFM) show decrease in the square root of the mean square values of roughness (RMS) when an increase the concentration of the solution. The transmittance started to appear above 550 nm, the increasing in concentration due to decreasing in transmition. The reflection spectrum of ($Fe_2O_3$) thin films increasing with increase concentration. Energy gap for direct transmission allowed an increase whenever increase concentration of the solution. The forward current of Photodetector is very small at voltage less than (2 V). the reversed current-voltage characteristics of the device measured in dark and the photocurrent under tungsten lamp illumination having two reversed current, the first area is located within the (2.5 Volt) in the case of concentration (0.05M) , (2 Volt) in the case of concentration (0.075M) and (0.7 Volt) in the case of concentration (0.1M) and the resultant from recombination current , While we note that the second region at high voltage represented the diffusion current. the value of the efficiency of the solar cell when the molarity conce-ntration (0.1M) greatest value was of (1.398%) , while the value of the solar cell efficiency when the molarity concentration (0.05M) was (1.065%).

**References**:

[1] Dr. P. Jayakumar ," Solar Energy Resource Assessment Handbook" September 2009

[2]Green, M. A. Silicon photovolt-aicmodules: a brief history of the first 50 years. Prog. Photovolt. Res. Appl. 13, 447– 455 (2005).

[3] Brus L. E. “Electron–electron and electron hole interactions in small semiconductor crystallites: The size dependence of the lowest excited electronic state” J. Chem. Phys. 80, 9 (1984) 4403.

[4] Dzhafarov T. D., Ongul F., Yuksel S.A.,” Effect of indium diffusion on characteristics of CdS films and nCdS/pSi heterojunctions”, 84, 2, (2010) 310.

[5] Aroutiounian V M, Arakelyan V M, Shahnazaryan G E,et al. Photoele-ctrochemistry of semiconductor electrodes made of solid solutions in the system Fe2O3–Nb2O5. Solar Energy,2006, 80: 1098

[6] Goodenough J B. Metallic oxides. Pergamon Press Ltd, 1971

[7] H. G. Cha, C. W. Kim, Y. H. Kim, M. H. Jung, E. S. Ji, B. K. Das, J.C. Kim and Y. S. Kang, "Preparation and characterization of α-Fe2O3 Nanorod-Thin Film by Metal-Organic Chemical Vapor Deposition" Thin Solid Films, 517, (2009) 1853

[8] M. Allen, D. Willits, J. Mosolf and M. Young, "Protein Cage Constrained Synthesis of Ferromagnetic Iron Oxide Nanoparticles" Adv. Mater, 14, (2002) 1562.

[9] B. L. Sharma and R. K. Purohit, "Semiconductor Heterojunctions", 1st Edition. Pergamon Press Ltd, NewYork, (1974).

[10] S. M. Sze, "Physics of Semiconductor Devices", 3rd Edition. John Wiley and Sons, Inc Publication, Canada, (2007).